# Accelerated Evolution of Tissue-Specific Genes Mediates Divergence Amidst Gene Flow in European Green Lizards

Sree Rohit Raj Kolora [1,2,3,4,*], Deisy Morselli Gysi[2,5,6], Stefan Schaffer[1,3], Annegret Grimm-Seyfarth[7], Márton Szabolcs[8], Rui Faria[9], Klaus Henle[1,7], Peter F. Stadler[1,2,10,11,12,13,14], Martin Schlegel[1,3], and Katja Nowick [15,*]

[1]German Centre for Integrative Biodiversity Research (iDiv) Halle Jena Leipzig, Leipzig, Germany

[2]Bioinformatics Group, Department of Computer Science, and Interdisciplinary Center for Bioinformatics, Universität Leipzig, Leipzig, Germany

[3]Molecular Evolution & Animal Systematics, University of Leipzig, Leipzig, Germany

[4]Department of Integrative Biology, University of California, Berkeley, Berkeley, CA, USA

[5]Swarm Intelligence and Complex Systems Group, Faculty of Mathematics and Computer Science, University of Leipzig, Leipzig, Germany

[6]Center for Complex Networks Research, Northeastern University, Boston, MA, USA

[7]Department of Conservation Biology, UFZ—Helmholtz Centre for Environmental Research, Leipzig, Germany

[8]Department of Tisza River Research, Danube Research Institute, Centre for Ecological Research, Hungarian Academy of Sciences, Debrecen, Hungary

[9]CIBIO, Centro de Investigação em Biodiversidade e Recursos Genéticos, InBIO, Laboratório Associado, Universidade do Porto, Vairão, Portugal

[10]Competence Center for Scalable Data Services and Solutions Dresden/Leipzig, Universität Leipzig, Leipzig, Germany

[11]Max-Planck-Institute for Mathematics in the Sciences, Leipzig, Germany

[12]Department of Theoretical Chemistry, University of Vienna, Wien, Austria

[13]Facultad de Ciencias, Universidad Nacional de Colombia, Bogotá, Colombia

[14]Santa Fe Institute, New Mexico, USA

[15]Institute for Biology, Freie Universität Berlin, Berlin, Germany

*Corresponding authors: E-mails: rohit@bioinf.uni-leipzig.de; katja.nowick@fu-berlin.de

## Abstract

The European green lizards of the *Lacerta viridis* complex consist of two closely related species, *L. viridis* and *Lacerta bilineata* that split less than 7 million years ago in the presence of gene flow. Recently, a third lineage, referred to as the "Adriatic" was described within the *L. viridis* complex distributed from Slovenia to Greece. However, whether gene flow between the Adriatic lineage and *L. viridis* or *L. bilineata* has occurred and the evolutionary processes involved in their diversification are currently unknown. We hypothesized that divergence occurred in the presence of gene flow between multiple lineages and involved tissue-specific gene evolution. In this study, we sequenced the whole genome of an individual of the Adriatic lineage and tested for the presence of gene flow amongst *L. viridis*, *L. bilineata*, and Adriatic. Additionally, we sequenced transcriptomes from multiple tissues to understand tissue-specific effects. The species tree supports that the Adriatic lineage is a sister taxon to *L. bilineata*. We detected gene flow between the Adriatic lineage and *L. viridis* suggesting that the evolutionary history of the *L. viridis* complex is likely shaped by gene flow. Interestingly, we observed topological differences between the autosomal and Z-chromosome phylogenies with a few fast evolving genes on the Z-chromosome. Genes highly expressed in the ovaries and strongly co-expressed in the brain experienced accelerated evolution presumably contributing to establishing reproductive isolation in the *L. viridis* complex.

**Key words:** genome, transcriptomes, gene flow, tissue-specific evolution, diversification, *Lacerta bilineata*, *Lacerta viridis*, Adriatic lineage.

## Significance

The *Lacerta viridis* species complex consists of multiple lineages across Europe. However, their evolutionary history and factors contributing to their divergence remain unclear. We found that the three lacertid lineages diverged recently in the past 2.2–7.6 million years with accelerated evolution in a few genes on the Z chromosome, in genes with high expression in the ovaries, and in genes with specific co-expression in the brain. Hence, this study shows that lacertid divergence has occurred amidst gene flow in combination with faster evolution of genes specifically expressed in brain and ovaries.

## Introduction

Comparative genomic studies, particularly between closely related species, provide an opportunity to identify changes at the genome level underlying adaptation and diversification (Dawson et al. 2002; Alföldi and Lindblad-Toh 2013). In particular, they allow shedding light on how divergence and speciation occur in the presence of gene flow, a process not yet well understood. During speciation, multiple reproductive barriers usually accumulate between populations making it increasingly unlikely for individuals of diverging populations to produce fertile or viable offsprings (Smadja and Butlin 2011). Postzygotic isolation caused by intrinsic incompatibilities has been pointed out as a relatively common barrier to gene flow between some species pairs that come into secondary contact, reflected in fitness disadvantage of interspecific hybrids (Coughlan and Matute 2020). Intrinsic incompatibilities often involve loci located in sex chromosomes and according to Haldane's rule, sterility and inviability should be more likely observed in the heterogametic sex (Schilthuizen et al. 2011). Possible reasons for this effect include the faster evolution of X-linked genes; dominance, because many incompatible alleles are recessive and mostly manifest in hybrids of the heterogametic sex; faster-male evolution, when hybrid male sterility evolves faster than inviability or female sterility and meiotic drive (Masly and Presgraves 2007). In the particular case of the faster-male theory, according to Masly and Presgraves (2007), two main causes have been suggested: sexual selection and the particular sensitivity of spermatogenesis that can be easily disrupted in hybrids. Studies on evolutionary rates in sex chromosomes are now relatively common; however, the majority involve XY sex determining systems. To our knowledge, whether an analogous "faster-female" effect potentially caused by easy disruption of hybrid oogenesis is common in ZW systems remains unknown. Deleterious interactions of transcription factors with DNA in hybrids could lead to considerable alterations of gene expression patterns, affecting one or multiple tissues, potentially hampering developmental programs or behavior. Hence, studying diverging expression patterns can be an important piece of information for genomic studies on speciation, providing a more completeunderstanding of the processes involved (Nowick et al. 2013).Lizards are interesting vertebrate models for evolutionary and ecological studies with multiple clades well-characterized in morphology, phylogeography, and varied modes of speciation (Camargo et al. 2010). In particular, *Lacerta bilineata* to *Lacerta viridis* are interesting models for studying genetic factors involved in speciation. These two taxa started to diverge less than 6 million years ago (Ma) with majorly unidirectional gene flow from the former to latter (Kolora et al. 2018). Extensive crossing experiments between *L. bilineata* and *L. viridis* showed reduced fitness of F1, F2, and F3 hybrids (majorly in heterogametic females) probably due to intrinsic incompatibilities, resulting in substantial reproductive isolation (Rykena 1991). Strikingly, recent phylogeographic studies detected two additional deep branching lineages including one in the previously described Slovenian hybrid zone between *L. bilineata* and *L. viridis*, referred to as the West Balkan (Böhme et al. 2007) or Adriatic lineage (Marzahn et al. 2016). Thus, the process of divergence within the *L. viridis* complex is more intricated than previously assumed. In particular, individuals from the Slovenian hybrid zone may not simply represent a contact between *L. bilineata* and *L. viridis* as previously thought, but comprise three divergent lineages: *L. bilineata*, *L. viridis*, and the Adriatic lineage. Consequently, their divergence must be analyzed together. In order to clarify the process of divergence between these lineages, including whether this occurred in the presence of gene flow, here we sequenced the whole genome of an individual of the Adriatic lineage and analyzed it with the genomes of *L. viridis* and *L. bilineata* we previously assembled (Kolora et al. 2018).

Within metazoans, diverging species exhibit lineage-specific differential gene expression patterns, as shown in *Drosophila* populations and house mouse species (Voolstra et al. 2007; Zhao et al. 2015). Differential gene expression is known to be consistently tissue-specific among different species across vertebrates (Sudmant et al. 2015; Wang et al. 2020). Furthermore, varying rates of evolution have been detected across tissues in humans and chimpanzees, with genes expressed in testes displaying on average higher rates of nonsynonymous substitutions per site relative to synonymous substitutions per site (Ka/Ks values) than genes expressed elsewhere (Khaitovich et al. 2005). In XY sex-determination systems, genes highly expressed exclusively in testis experience faster rates of evolution than other genes. In ZW-mediated systems, the role of tissue-specific genes in species divergence is an active area of research. Interestingly, in
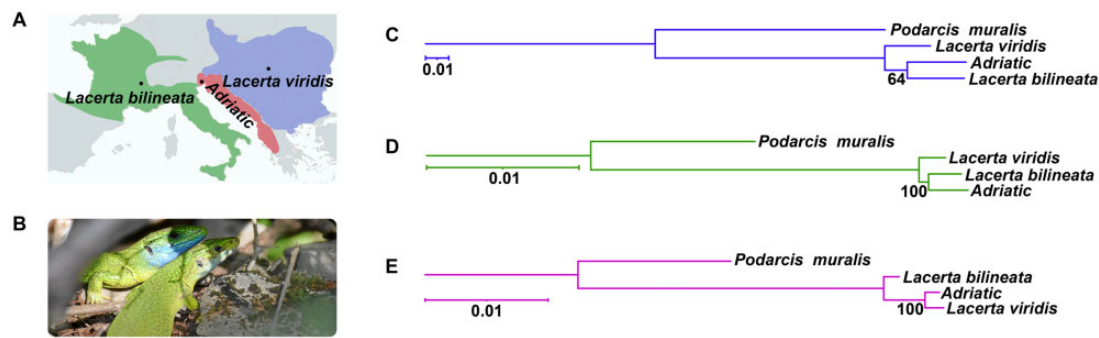
FIG. 1.—(A) Distribution map of *L. viridis*, *L. bilineata*, and the Adriatic lineage across Europe (adapted from Marzahn et al. 2016) (sampling locations are highlighted with dots). (B) Adult male (more prominent blue throat) and female (both identified as Adriatic lineage) in their natural habitat in Slovenia. The phylogenetic tree constructed using the concatenated coding sequences of the (C) mitochondrial genes, (D) autosomal genes, and (E) genes on the Z chromosome with *P. muralis* as the outgroup.

the *L. viridis* complex, genes experiencing varying levels of positive selection are enriched for transcriptional and splicing-related activities (Kolora et al. 2018), raising the question to which extent expression patterns differ among these lineages and whether genes specifically expressed in certain tissues are fast evolving.

In order to understand the evolutionary history of the *L. viridis* complex, we used sequencing data from the whole mitogenome, autosomes, and Z chromosome to reconstruct the phylogeny of three *L. viridis* complex lineages and detect gene flow during their divergence. Our results suggest that the Adriatic lineage and *L. bilineata* are sister taxa and the presence of admixture between these lineages of the *L. viridis* complex. We further sequenced the transcriptomes of five different tissues to test for tissue-specific evolution. The divergence of these lineages is accompanied by accelerated evolution of genes with specific expression patterns in brain and ovaries.

## Results and Discussion

### Evolutionary History of the *Lacerta viridis* Complex

In our phylogenetic tree based on mitogenomes, the Adriatic lineage clustered with *L. bilineata* with a relatively low (64) bootstrap support (fig. 1C). This indicates lower divergence between the Adriatic lineage and *L. bilineata* with maternally inherited markers. The same topology is also observed in the autosomal tree but with higher support (100) (fig. 1D). However, the tree based on genes from the Z chromosome shows a topology where *L. viridis* and Adriatic cluster together, also with strong (100) support (fig. 1E). Possible explanations for this difference in topology include sample size for the sex chromosome gene orthologs ($n = 12$), sex-biased gene flow, introgression on the sex chromosome, sexual selection, genetic incompatibilities, or reduced effective population size and lower recombination rates on the Z chromosomes (Wilson Sayres 2018).

Based on the autosomal time calibrated tree, the divergence between *L. viridis* and *L. bilineata*/Adriatic as 4.9($\pm$2.7) million years ago (Ma). The divergence time between *L. bilineata* and the Adriatic lineage was 2.27($\pm$1.3) Ma, while the ancestor of *Lacerta* split from *Podarcis* 33.5($\pm$18.9) Ma. These divergence time estimates are in line with previous studies that reported divergence between *L. viridis* and *L. bilineata* to have occurred between 1.2 and 3 Ma (Kolora et al. 2018) while accounting for gene flow during divergence and 6.8 Ma (Sagonas et al. 2014) when not accounting for gene flow. The unrooted species tree generated from the multi-species coalescent model, which accounts for incomplete lineage sorting (ILS), generated a species tree topology identical to the autosomal tree at high confidence (probability of 1).

We applied D-statistics, a formal test of admixture given a four population phylogeny to infer possible gene flow by measuring allele sharing among the lineages. Here, we computed D-statistics assuming a species tree structure of D(W, X, Y, Z) where we assume *Podarcis muralis* as the outgroup Z. Our D-statistic results from both autosomes and Z-chromosome data support the presence of gene flow between *L. viridis* and Adriatic (table 1). Since there was previous evidence for gene flow between *L. viridis* and *L. bilineata* (Kolora et al. 2018), altogether this indicates admixture between all three lineages of the *L. viridis* complex.

The presence of contact zones with possible gene flow between *L. viridis* and *L. bilineata* was proposed in the geographic region currently inhabited by the Adriatic lineage (Godinho et al. 2005). More recent studies based on the mitochondrial DNA (mtDNA) proposed a distinct lineage status for the Adriatic lineage (Böhme et al. 2007; Marzahn et al. 2016). Our phylogenetic tree suggests that the Adriatic lineage is a sister taxon to *L. bilineata* and admixture tests support that gene flow occurred during divergence between the *Lacerta* lineages.

Hybridization experiments between lineages of the *L. viridis* complex showed that sterility in female hybrids was higher

Gene Flow on Autosomes and Z-Chromosome within the *L. viridis* Complex with *P. muralis* as the Outgroup

| Lineage1 | Lineage2 | Lineage3 | Outgroup | Autosomes | | Z-chromosome | |
|----------|----------|----------|----------|-----------|--------|--------------|--------|
| | | | | Dstat | Z-score | Dstat | Z-score |
| *L. bilineata* | **Adriatic** | *L. viridis* | *P. muralis* | −0.242 | −79.326 | −0.311 | −13.794 |

NOTE.—Negative values indicate gene flow between Lineage 2 and Lineage 3. Lineages experiencing gene flow on autosomes and Z-chromosome are highlighted in bold.
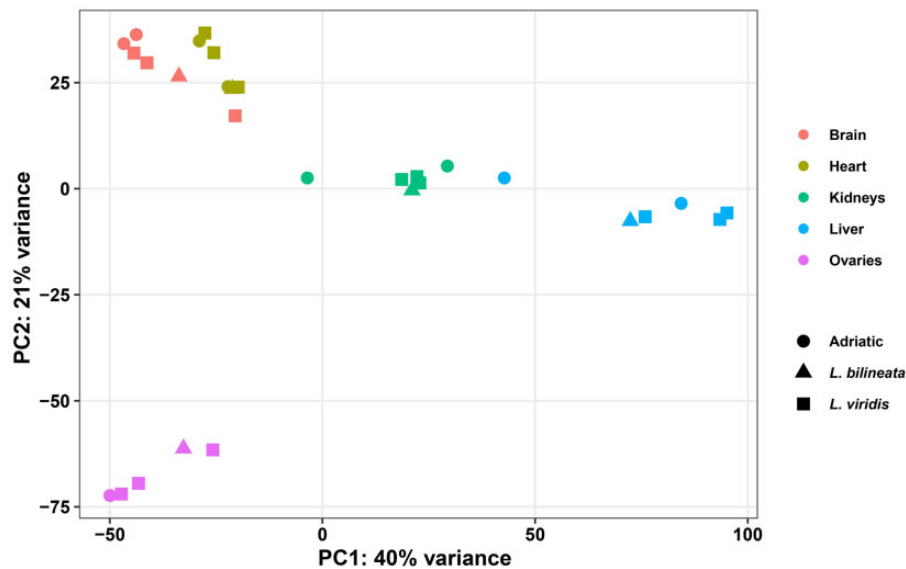


FIG. 2.—Clustering of samples based on their gene expression differences among samples. The lineage names (*L. viridis*, *L. bilineata*, and Adriatic) are represented by the shapes and the tissues by colors. The plot has been generated based on variance-stabilizing transformations in DESeq2.

than in male hybrids (sterility of 4% in F1 females and <1% in males) (Rykena 1991). Reproductive barriers among lineages manifested in F1s and later generation hybrids (Rykena 1991) could have been caused by incompatibilities involving some genes on the Z-chromosome. Since gene flow occurred during the divergence between these, we speculate that reinforcement could have strengthened reproductive isolation between lineages. Assortative mating occurs within populations of *L. viridis* with females preferring males with higher UV reflectance on the throat (Bajer et al. 2010). Blue color of the throat and UV reflectance in males as well as the yellow chest in females are regarded as honest signals of fitness (Molnár et al. 2016). Assortative mating and fitness differences in females could have led to different evolutionary histories across autosomes and sex chromosomes eventually contributing to divergence between these species/lineages. Since the existence of the Adriatic lineage was unknown until recently (i.e., cryptic species), the reproductive barriers between the Adriatic lineage and the other two species are currently uncertain. Further studies are needed to identify the main reproductive barriers between this trio of species, as well as the underlying genomic regions (i.e., barrier loci) and their distribution across the genome.

### Tissue-Specific Evolution in the *Lacerta viridis* Complex

Based on gene expression differences, samples cluster clearly by tissues rather than lineage with the exception of an Adriatic liver sample which was removed from subsequent analysis (fig. 2, supplementary fig. S1, Supplementary Material online). The first two principal components (PC1 and PC2) explained 61% of variance in gene expression and ovaries exhibit the highest level of variance compared to other tissues. Similarly, in flycatchers (ZW system), the highest gene expression variance was observed in ovaries (Uebbing et al. 2016).

Tissue-specific genes were defined as genes with significantly higher expression in one tissue compared to the other tissues (see Materials and Methods section). By far, the highest number of tissue-specific expressed genes were detected in ovaries (1066 genes), almost twice compared to the second tissue, brain (supplementary table S2, Supplementary Material online). Ovaries also had more genes with high log fold change (LFC) values than the other tissues (supplementary fig. S2A, Supplementary Material online). As expected, brain-specific genes were over-represented for genes involved in neural development and synaptic transmission, heart for circulatory processes and myofibril activity, liver for catabolic

**Table 2**

Result of the Tests Comparing Evolutionary Rates (between *L. viridis* and *L. bilineata*) for Genes Differentially Expressed in a Specific Tissue versus those without Tissue-Specific Expression

| Tissue | #Tissue genes tested | #Background genes | MWU test (P value) | BH (q value) |
|---|---|---|---|---|
| Brain | 316 | 9524 | 0.505 | 0.504 |
| Heart | 197 | 9643 | 0.271 | 0.338 |
| Liver | 400 | 9440 | 1.5e−05 | **6e−04** |
| Kidneys | 27 | 9813 | 0.0141 | **0.0235** |
| Ovaries | 1066 | 8774 | <1e−06 | **<1e−06** |

Note.—One sided (alternative = greater) Mann–Whitney U test (MWU) was performed to compare significant differences in evolutionary rates followed by multiple testing using the Benjamini–Hochberg (BH) method. Significant results ($q < 0.05$) are highlighted in bold.

processes and peptidase activity, and ovary-specific genes were enriched for cell division and DNA synthesis processes (supplementary table S3, Supplementary Material online), indicating that gene sets are indeed enriched for tissue-specific genes. Only kidney-specific genes did not exhibit any tissue-specific gene ontology (GO) over-representation, which could be a caveat of fewer genes with significantly higher expression in kidneys.

Ubiquitously expressed genes (i.e., classified as unspecific to any tissue) showed the highest frequency of slow evolving genes (supplementary fig. S2*B*, Supplementary Material online). Comparing evolutionary rates between *L. viridis* and *L. bilineata* among tissue specifically expressed genes revealed that ovaries had a more skewed distribution toward fast evolving genes when compared to background genes (table 2).

Genetic incompatibilities between species can accumulate on the heterogametic sex chromosomes, which are retained due to lower recombination rates compared to autosomes (Johnson and Lachance 2012). On the Z-chromosome, we detected three genes (CHRDL1, ERCC6L, and MTM1) with signatures of rapid evolution ($\omega > 1$) and also involved with sex-linked functions. Mutated CHRDL1 genes have been shown to cause X-linked megalocornea in humans and African clawed frogs (Pfirrmann et al. 2015). Mutations in ERCC6L affect chromosomal segregation (Hutchins et al. 2010) and in MTM1 cause X-linked myopathy (Cowling et al. 2014). Our finding that many ovary-specific genes showed accelerated evolution (ZW sex determination system) is in line with testis-specifically expressed genes evolving faster in primates (XY sex deterministic system) (Khaitovich et al. 2005), since in both lineages genes specifically expressed in the gonads of the heterogametic sex-specific tissue seems to evolve faster. In anoles (XY sex determination system), genes related to reproductive functions also experience accelerated evolution (Tollis et al. 2018). As previously stated, sexual selection can drive rapid sequence divergence in genes on the Z-chromosome or genes specifically expressed in reproductive

organs. Alternatively, this pattern can arise if oogenesis can be easily perturbed in hybrid females, as reported in the heterogametic female progeny between *L. viridis* and *L. bilineata* (Rykena 1991). It could be hypothesized that some of the rapidly evolving genes expressed in ovaries are involved in incompatibilities that manifest in hybrids of heterogametic sex, specifically affecting ovarian function/development. Although it was previously shown that a higher percentage of hybrid females between *L. bilineata* and *L. viridis* are sterile or inviable than males (Rykena 1991), the link between accelerated evolution in ovaries expressed genes, incompatibilities and misexpression in hybrid individuals still needs to be tested by studying hybrid individuals in the future.

To further shed light on the evolution of more complex traits, we analyzed co-expression networks of each tissue. These networks capture potential interactions among gene products which can be altered due to sequence and/or expression differences. The brain gene co-expression network was characterized by the highest weighted topological overlap (wTO) values and connectivity, followed by heart and ovaries (supplementary fig. S3, Supplementary Material online). This suggests stronger gene co-expression in the brain compared to other tissues. The total number of tissue-specific links, as well as the number of links shared by a specific tissue with any other tissues are listed in supplementary table S5, Supplementary Material online. Liver, brain, and heart had the most tissue-specific links, followed by ovaries (supplementary fig. S4, table S4, Supplementary Material online), which agrees with the higher connectivity observed in these tissues, apart from liver, a trend similar to that observed in mice (Mack et al. 2019). We detected 12,100 genes with tissue-specific network integration, that is, genes that displayed a significantly higher number of tissue-specific links in any of the tissues (supplementary table S5, Supplementary Material online). The tissue-specific co-expression networks from the brain and liver were the densest whereas kidneys showed the least dense co-expression network (fig. 3). Two clearly separated clusters were observed in the networks of all tissues, except kidneys (potentially due to its sparsity). For all tissues, we found a significant positive association between tissue-specifically expressed genes (from differential expression analysis) and tissue-specifically co-expressed genes (supplementary table S5, Supplementary Material online). We did not observe any functional enrichments in either one of the gene clusters for any tissue. However, the bi-modularity in these co-expression networks is based on the direction of expression, that is, up- or downregulation of genes (supplementary fig. S5, Supplementary Material online).

Genes co-expressed specifically in the brain are most skewed toward faster evolutionary rates compared to other tissues (table 3). Given the positive association between tissue-specific expression and evolutionary rates, it is possible that fast-evolving genes are forming tissue-specific co-expression modules especially in the brain. Genes coding for
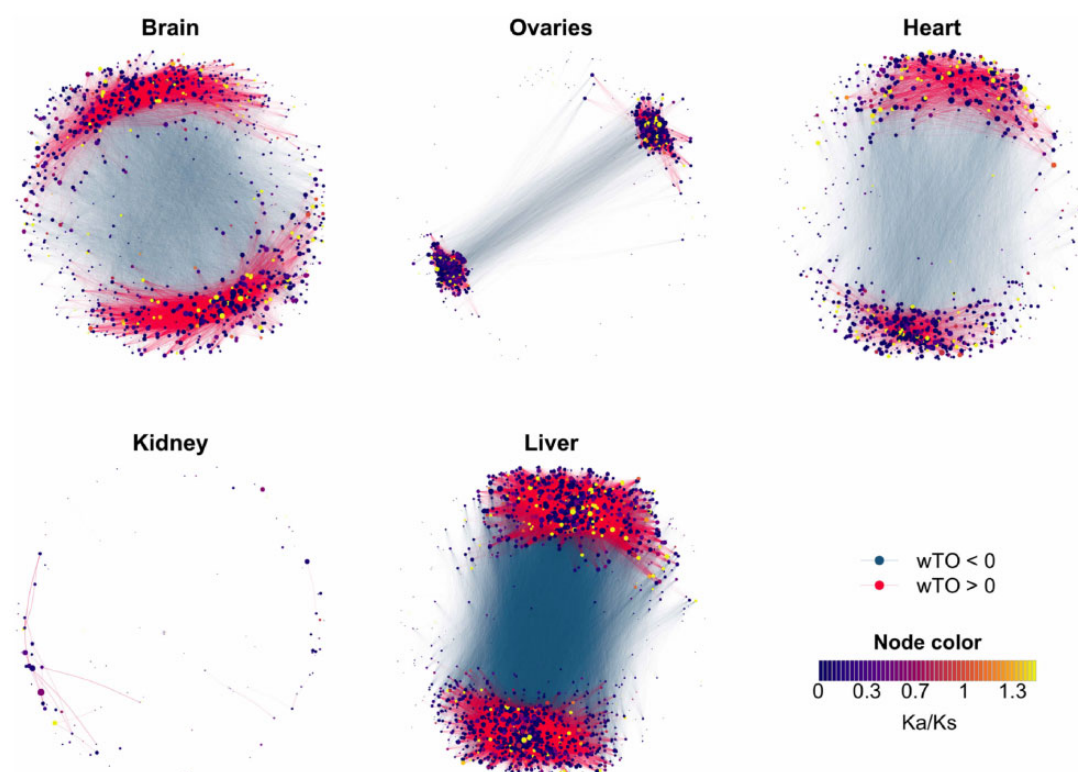
**Fig. 3.**—Gene co-expression networks across different tissues with different rates of evolution ($\omega$ = Ka/Ks). Genes in kidneys were very sparsely connected compared to other tissues. Positive relationships between genes are shown as red and negative relationships as blue links. Networks are bimodular, with positive links primarily within modules and negative links between modules. The colors of the nodes indicate their Ka/Ks value.

**Table 3**

Results of the Tests Comparing Evolutionary Rates (between *L. viridis* and *L. bilineata*) for Tissue-Specifically Co-Expressed Genes versus those without Significant Co-Expression in that tissue

| Tissues | #Tested genes | #Background genes | MWU test (P value) | BH (q value) |
|---|---|---|---|---|
| Brain | 1116 | 8674 | <1e−06 | **<1e−06** |
| Heart | 937 | 8903 | 0.026 | **0.043** |
| Liver | 1713 | 8127 | 0.104 | 0.130 |
| Kidneys | 224 | 9616 | 0.010 | **0.026** |
| Ovaries | 885 | 8955 | 0.251 | 0.251 |

NOTE.—Significant q-values are highlighted in bold.

transcription factors are among those genes with high $\omega$ values, for example, *NOVA-1* and the gene silencing protein Histone *H2A*. We speculate that brain-specific genes without faster rates of evolution at the sequence level themselves might be influenced in their expression patterns by such transcription factors and other accelerated genes. In other words, fast evolving genes seem to influence expression patterns of genes specifically co-expressed in the brain. Notably, and in contrast to general expectation and the other tissues, the strength of nodes is positively correlated with their $\omega$ value in the brain. This means that genes experiencing more relaxed

purifying selection or positive selection tend to have more links to other genes in the brain co-expression network (all fast evolving genes are listed in supplementary table S6, Supplementary Material online). Their influence on other genes is higher than expected by chance (GLM binomial family, exp(beta) = 1.0004, *P* < 0.001).

Rewiring of co-expression networks has also been observed in primate brains (Berto and Nowick 2018). In our data, genes especially involved in gene regulation (*MXD3*, *MYBL2*, *NOVA1* and *SPIC*), developmental processes (*APBA1*, *MTM1*, *NEUROD6*, *LRTM2*, *SCN1B* and VAMP1), cognitive (*CHRDL1* and *MLC1*), and reproductive functions (ASTL, ERCC6L, MASTL, and MCM9) underwent changes in network connectivity among the three lineages. In summary, based on transcriptomic data we observed significantly faster evolution in genes with ovary and brain-specific (co-)expression patterns. It is tempting to speculate that the evolutionary changes in their co-expression networks underlie behavioral changes leading to reproductive isolation.

In summary, we studied the evolutionary history of the *L. viridis* complex by reconstructing the phylogeny and detecting gene flow between its lineages using whole-genome data, where we estimated a mean divergence time of 2.27 Ma between the Adriatic lineage and *L. bilineata* and 4.9 Ma

between *L. viridis* and *L. bilineata*/Adriatic lineage. We also detected gene flow between *L. viridis* and the Adriatic in addition to the previously known gene flow between *L. viridis* and *L. bilineata* (Kolora et al. 2018). Our analyses of tissue-specific genes revealed faster evolution in a few genes on the Z-chromosome in addition to genes highly expressed in ovaries, concordant with observations across other vertebrates (Khaitovich et al. 2005; Tollis et al. 2018). We can gain a better understanding of species evolution within vertebrates in general by accounting for genetic variation in a phylogenetic context (Chen et al. 2019). Our work explored the phylogeny of the *L. viridis* complex at a whole-genome level compared to previous studies focusing on a handful of markers (Sagonas et al. 2014; Marzahn et al. 2016). However, we note that future studies with multi-population data would greatly help tease apart complex demographic scenarios and direction/degree of gene flow within the species complex of European green lizards.

## Conclusions

The evolutionary history of the *L. viridis* complex seems to have been shaped by gene flow. Our study not only confirms the existence of a distinct Adriatic lineage as a sister group to *L. bilineata* but also suggests admixture with *L. viridis*. Multiple factors including fitness differences between hybrid females and males and eventually assortative mating could have led to different evolutionary histories across autosomes and sex chromosomes. Evolutionary changes have most impacted genes majorly expressed in ovaries and genes strongly co-expressed in the brain. Faster evolution could have resulted in incompatibilities disrupting gene function in ovaries and more complex gene expression differences probably occurred in the brain during speciation amidst gene flow in the *L. viridis* complex.

## Materials and Methods

### Sampling Scheme, Genome and Transcriptome Sequencing

Animals (two female *L. viridis* from Hungary, one female *L. bilineata* from France, one male, and one female Adriatic specimen from Slovenia—see supplementary table S1, Supplementary Material online for detailed locations and sampling period) were captured with permits of the issuing authorities (see Acknowledgements) and handled according to the guidelines of the Herpetological Animal Care and Use Committee of the American Society of Ichthyologists and Herpetologists. Brain, heart, liver, kidney, and ovaries were dissected for tissue-specific transcriptome sequencing, and the remaining tissues were stored separately at −80°C.

For the whole-genome sequencing of the female Adriatic specimen, tail tissue was digested with proteinase K and a chloroform-based method was used to extract the whole genomic DNA. Short-read libraries with insert sizes of 450 bp were prepared. The Illumina paired-end sequences were double-indexed using a multiplexing sequencing protocol (Meyer and Kircher 2010) and sequenced on a HiSeq2500.

In the case of transcriptome sequencing, Trizol Reagent (Life Technologies, Carlsbad, CA, USA) was used to extract the RNA from each tissue which was later purified with the RNeasy Mini Kit (Qiagen, Hilden, Germany) and Dynabeads mRNA Purification Kit (Life Technologies). Ambion RNA fragmentation reagent was used to obtain 200–250 bp fragments. Random hexamers with SuperScript II reverse transcriptase (Life Technologies) and DNA Polymerase I with RNase H treatment (Life Technologies) were used to synthesize the first and second strands of complementary DNA (cDNA), respectively. Similar to the genomes, the cDNA was double-indexed and paired-end sequenced on an Illumina HiSeq2500.

### Sequencing Data Processing and Mitogenome Assembly

The whole-genome sequencing reads of Adriatic sample were trimmed using cutadapt (Martin 2011) with a minimum length of 30 and match-read-wildcards option for the following adaptor sequences:

- GATCGGAAGAGCACACGTCTGAACTCCAGTCACNNNN NNATCTCGTATGCCGTCTTCTGCTTG
- GATCGGAAGAGCGTCGTGTAGGGAAAGAGTGTACATC TCGGTGGTCGCCGTATCATT

The Illumina paired end reads were corrected using MUSKET tool (V1.1) (Liu et al. 2013) with a kmer size of 21 and the overlapping ends of paired reads were merged with a minimum overlap of 30, maximum overlap of 75 and error rate of 0.015 using FLASH (V1.2.11) (Magoc and Salzberg 2011). These overlapping and non-overlapping paired end reads were assembled *de novo* with Minia assembler (V2.0.7) (Chikhi and Rizk 2013) using a kmer size of 81 and minimum kmer coverage of 3. The contigs from the genome assembly were aligned to the *L. bilineata* and *L. viridis* mitogenomes (KT722705 and NC_008328.1, respectively) using BWA MEM (V0.7-15) (Li 2013). The mitogenomic contigs were combined with a minimum overlap of 30 bases and 90% identity using CAP3 assembler (Huang and Madan 1999) to recover the whole mitogenome. The mitogenome was annotated using MITOS (Bernt et al. 2013).

### Genome Mapping, SNP Calling and Filtering

The paired-end Illumina reads from *L. viridis* (ERS2087156) and *L. bilineata* (ERS2087829), Adriatic lineage (ERS4631750) and *P. muralis* (SAMN10820182) were aligned to the chromosome level of the *P. muralis* reference genome with the short read alignment tool BWA MEM and the alignments were sorted with Samtools (V1.8) (Li et al. 2009). After preprocessing, the variants were called using haplotype caller

of the Genome Analysis Toolkit (GATK V4) (McKenna et al. 2010) followed by variant filtering based on GATK best practices protocol (duplicates marked, indels realigned and filter for minimum mapping quality of 20 and minimum read depth of 8). This retained 26,985,663 SNPs for autosomes (Chr1 to Chr18 in *P. muralis*) and 720,884 bi-allelic SNPs in the Z chromosome for subsequent analyses.

## Admixture Test

To test for the presence of gene flow between lineage pairs, we used D-statistics. D-statistic is a powerful test to detect a genome-wide signal of introgression rather than local regions of introgression in the genome. The genome-wide estimates of D-statistic were calculated using AdmixTools (Patterson et al. 2012) with *P. muralis* as outgroup based on the species tree topology. D-statistic is a formal test of introgression between randomly mating populations (three populations P1, P2, P3 and an outgroup O) using genome-scale SNP data from ancestral (A) and derived alleles (B). The null hypothesis is absence of gene flow with equally frequent "ABBA" and "BABA" allelic patterns, while significant introgression ($Z < -3$ or $Z > 3$) is evident from an excess in either ABBA (negative D-statistic, gene flow between P2 and P3) or BABA (positive D-statistic, gene flow between P1 and P3) patterns.

## RNAseq Data Processing

The RNAseq data from the sequenced Adriatic ($n = 2$, one male and female), *L. viridis* ($n = 2$, both females), and *L. bilineata* ($n = 1$, one female) samples (five tissues each) were adaptor trimmed using cutadapt with the adaptors and options identical to the genomic reads. The RNAseq reads were aligned to the *L. viridis* reference genome using STAR aligner (Dobin et al. 2013) with splicing specific parameters permissive to mismatches and indels (-A 85 -Z 20 -S). The RNAseq alignments from STAR were used to count the reads mapping to each genomic feature (here genes) using featureCounts of the Subread package (V1.5.1) (Liao et al. 2014). Multiple mapping positions were allowed for the reads. Only gonads from the female samples were used in gene expression analysis of reproductive tissues due to absence of biological replicates for male gonads.

## Transcriptome Assembly and Gene Orthology

The overlapping paired-end reads from adapter trimmed RNAseq data were merged using FLASH. The transcripts were de novo assembled separately for each tissue from the two individuals of Adriatic lineage (10 transcript assemblies) and for five tissues of the female *L. viridis* (five transcript assemblies) using Trinity (Grabherr et al. 2011) with reads normalized to maximum coverage of 80. The assembled transcripts were queried for open reading frames and the protein coding sequences were extracted using Transdecoder of the Trinotate pipeline (Bryant et al. 2017) with a minimum log-likelihood score of 10. The transcripts for *L. bilineata* were downloaded from the existing assembly data set (Kolora et al. 2018).

For Adriatic lineage transcripts, the longest transcripts, which aligned in similar synteny to both *L. viridis* and *L. bilineata* reference genomes, were retained based on GMAP alignments (V2016-08-24) (Wu et al. 2016) adjusted for best alignments only (-n 1) and cross species parameters (-Y). Orthologs were identified using ProteinOrtho5 (Lechner et al. 2011) with an identity threshold of 70%, e-value cutoff of $10^{-6}$ and the synteny information of gene positions with *P. muralis* as an outgroup. Only the single copy orthologs (SCOs) were used to test the rates of evolution.

## Phylogeny Reconstruction

The 13 protein coding DNA sequences (CDS) of the three *L. viridis* complex mitogenomes (*L. bilineata*: KT722705, *L. viridis*: NC_008328.1, Adriatic lineage: LR999461.1) were aligned along with *P. muralis* (NC_011607.1). Multiple sequence alignment (MSA) was performed for the CDS from the four taxa progressively with MAFFT tool (Katoh et al. 2002) using an iterative refinement method over 1000 iterations and trimming all alignment gaps with trimAL (V1.2) (Capella-Gutiérrez et al. 2009) to output a phylip format MSA. Since multiple concatenated genes were aligned, IQ-TREE2 (Minh et al. 2020) was used to reconstruct a maximum likelihood based phylogeny using partitioned alignments (https://github.com/ChrisCreevey/catsequences.git, Accessed July 16, 2020), automatic model selection and ultrafast bootstraps ($n = 1000$) with *P. muralis* as the outgroup. The same procedure was repeated for orthologous genes post-filtering from the autosomes (1497 genes) and Z-chromosomes (12 genes). We used a multispecies coalescent method for species tree estimation and divergence time calibration with the likelihood-based Bayesian model-selection implementation BPP (Flouri et al. 2020). This assumes no recombination among sites within a locus, neutral clock-like evolution and no gene flow between species. Although the BPP analysis is limited by the assumption of strict divergence without migration and strict clocks, it performs better for species tree estimation in the presence of ILS short internal branches (Shi and Yang 2018). We used the models A01 (assigned sequenced to species) for inferring species tree and A00 (parameter estimation under fixed phylogeny) to estimate species divergence times ($\tau_s$). Partitioned autosomal gene alignments (1497 loci) accounting for heterogeneity were input as diploid unphased sequences. Priors were provided for estimated theta (invgamma $a = 3$, $b = 0.006$ assuming a heterozygosity of 0.0008–0.009) with option 'e' for estimation for reducing parameter space and root-tau (invgamma $a = 3$, $b = 0.03$ based on calculated genome divergence of 1.5% between *L. viridis* and *Podarcis*). This was run for 1 million MCMC

samples for every two iterations and burnin of 4000. The best tree was used as a fixed phylogeny to estimate species divergence times with the same parameters using model A00. The coalescent trees were calibrated to divergence times assuming a mutation rate of 1e−9 and a generation time of 1.5–3.5 years (Kolora et al. 2018) using the workflow by Yoder et al. (2016) (https://github.com/mariodosreis/mousies, Accessed February 14, 2021). This workflow converts the coalescent branch length estimates obtained from BPP into geological times.

## Gene Expression Patterns

The R package DESeq2 (Love et al. 2014) was used to perform gene expression analysis based on read counts for genes in our RNA-Seq data. Tissue-specific gene expression patterns were identified by comparing each tissue against all other tissues, considering the biological specimens from the different taxa as replicates (five conditions: brain, heart, liver, kidneys, and ovaries) using the contrast option in DESeq2. The contrast option is a linear combination of estimated LFC used to test whether the compared groups are similar. If genes were highly expressed in only one tissue compared to all other tissues (LFC $\geq$ 1.5; intersected list), these were considered as expressed in tissue-specific manner.

## Gene co-Expression Network Analyses

To remove genes with little information with respect to gene expression patterns, genes with an average expression count and standard deviation lower than 1 were filtered out, thus retaining 12,716 genes for the co-expression network analysis.

Each tissue-specific co-expression network was constructed using normalized RNAseq data from all three lineages (L. bilineata = 1 individual, 5 tissues, 5 replicates; L. viridis = 2 individuals, 5 tissues, 10 replicates; Adriatic = 2 individuals, 5 tissues, 10 replicates). Networks were constructed using a modification of the wTO method (Langfelder and Horvath 2012), allowing both positive and negative interactions using the wTO R package that calculates a probability for each link (Gysi et al. 2018). The networks were constructed using Pearson correlations and 100 replicates for bootstrapping. Networks were filtered for keeping links with an absolute wTO value higher than 0.5 and BH adjusted P values smaller than 0.15; links below that threshold were set to zero.

In order to compare those networks across tissues, we used the co-expression differential network analysis method (CoDiNA) implemented as an R Package (Gysi et al. 2020). CoDiNA categorizes links (gene interactions) and nodes (genes) into three main categories: Common ($\alpha$), Different ($\alpha$), and Specific ($\gamma$). A link is said to be *common* if it is present in all networks and has the same sign in all networks. A link is defined as *different* if it is present in all networks but has a different sign in at least one network. Links are considered *specific* if they are only present in a subset of networks. A ratio of the CoDiNA scores of at least two was used for filtering to assure that all classified links were strong and well assigned to one of the categories. Only these strong and well classified links were retained for classification of the genes into Common ($\alpha$), Different ($\alpha$), and Specific ($\gamma$). Well classified genes were subsequently tested for GO enrichments and variation in the rates of evolution.

## GO-Enrichment Analysis

GO enrichment analyses were performed to identify biological functions and/or pathways that undergo tissue-specific expression. PantherDB (2018_04 release) (Mi et al. 2010) overrepresentation tests (release 20190711) were performed with different annotation data sets such as biological process, molecular functions, pathways, cellular components, and protein classes. Fisher's exact test was used to detect significant overrepresentations followed by multiple testing (FDR < 0.05).

## Rates of Evolution

SCOs from the orthogonal gene sets were retained to test for the rate of evolution between lineage pairs. The orthologs from lineage pairs were aligned with MACSE V2 (Ranwez et al. 2018) after removing stop codons and accounting for frame-shift mutations followed by alignment gap removal with trimAL (V1.2).

The ratio of nonsynonymous (Ka) to the synonymous (Ks) substitution rates(Ka/Ks), that is, the $\omega$ value within the SCOs, can be used to test for selection. $\omega = 1$ suggests neutral evolution, $\omega > 1$ positive or relaxed (diversifying) and $\omega < 1$ negative (purifying) selection. The synonymous and nonsynonymous sites were defined based on four-fold synonymous sites, and KaKs_Calculator 2.0 toolkit (Wang et al. 2010) was used to calculate $\omega$ based on different substitution models followed by model averaging (MA).

Differences in rates of evolution using $\omega$ values (between L. viridis and L. bilineata) were tested between genes with tissue-specific and non-tissue-specific expression. The rates of evolution were taken from the pairwise comparison of L. viridis and L. bilineata since they showed a higher number of SCOs (10,652 compared to <2500 with Adriatic lineage pairs). Their $\omega$ values were compared to those of the background (non-tissue-specific expression) using a one sided (alternative = greater) Mann–Whitney U test (unpaired) through the wilcox.test function in R (V3.5.2). Multiple testing was conducted by the BH method (option $pi0 = 1$) using the q value package (V2.14.1) (Storey et al. 2019).

## Supplementary Material

Supplementary data are available at *Genome Biology and Evolution* online.

## Acknowledgments

## Author Contributions

K.H., A.G.-S., and M.Sz. collected the samples; S.S. sequenced the genome and transcriptomes; S.R.R.K. performed the assembly, annotation, analysis of differential expression, selection and gene flow; D.M.G. analyzed the co-expression networks, S.R.R.K., K.N., K.H., P.F.S., and M.S. wrote the initial draft of the manuscript; D.M.G., M.Sz., S.S., and R.F. edited the manuscript; K.N., K.H., P.F.S., and M.S. conceived the study.

## Data Availability

All the sequencing data was deposited at European Nucleotide Archive the Study "PRJEB38736". Transcript assemblies, genome assembly, mitogenome annotation and variant calls are provided at https://doi.org/10.5281/zenodo.3900517.

## Literature Cited

Alföldi J, Lindblad-Toh K. 2013. Comparative genomics as a tool to understand evolution and disease. Genome Res. 23:1063–1068.

Bajer K, Molnár O, Török J, Herczeg G. 2010. Female European green lizards (*Lacerta viridis*) prefer males with high ultraviolet throat reflectance. Behav Ecol Sociobiol. 64(12):2007–2014.

Bernt M, et al. 2013. MITOS: improved de novo metazoan mitochondrial genome annotation. Mol Phylogenet Evol. 69:313–319.

Berto S, Nowick K. 2018. Species-specific changes in a primate transcription factor network provide insights into the molecular evolution of the primate prefrontal cortex O'Connell, M, editor. Genome Biol Evol. 10(8):2023–2036.

Böhme MU, et al. 2007. Phylogeography and cryptic variation within the *Lacerta viridis* complex (Lacertidae, Reptilia). Zool Scripta. 36(2):119–131.

Bryant DM, et al. 2017. A tissue-mapped axolotl de novo transcriptome enables identification of limb regeneration factors. Cell Rep. 18:762–776.

Camargo A, Sinervo B, Sites JW. 2010. Lizards as model organisms for linking phylogeographic and speciation studies. Mol Ecol. 19:3250–3270.

Capella-Gutiérrez S, Silla-Martínez JM, Gabaldón T. 2009. trimAl: a tool for automated alignment trimming in large-scale phylogenetic analyses. Bioinformatics 25:1972.

Chen L, et al. 2019. Large-scale ruminant genome sequencing provides insights into their evolution and distinct traits. Science 364(6446):eaav6202.

Chikhi R, Rizk G. 2013. Space-efficient and exact de Bruijn graph representation based on a Bloom filter. Algorithms Mol Biol. 8:22.

Coughlan JM, Matute DR. 2020. The importance of intrinsic postzygotic barriers throughout the speciation process. Philos Trans R Soc B Biol Sci. 375:20190533.

Cowling BS, et al. 2014. Reducing dynamin 2 expression rescues X-linked centronuclear myopathy. J Clin Invest. 124:1350–1363.

Dawson MN, Louie KD, Barlow M, Jacobs DK, Swift CC. 2002. Comparative phylogeography of sympatric sister species, *Clevelandia ios* and *Eucyclogobius newberryi* (Teleostei, Gobiidae), across the California Transition Zone. Mol Ecol. 11:1065–1075.

Dobin A, et al. 2013. STAR: ultrafast universal RNA-seq aligner. Bioinformatics 29:15–21.

FlouriT, RannalaB, Yang Z. 2020. A tutorial on the use of BPP for species tree estimation and species delimitation. In: Scornavacca C, Delsuc F, Galtier N, editors. Phylogenetics in the Genomic Era. No commercial publisher | Authors open access book p. 5.6:1–5.6:16. https://hal.archives-ouvertes.fr/hal-02536475 (Accessed February 10, 2021).

Godinho R, Crespo E, Ferrand N, Harris DJ. 2005. Phylogeny and evolution of the green lizards, *Lacerta* spp. (Squamata: Lacertidae) based on mitochondrial and nuclear DNA sequences. Amphib Reptilia. 26(3):271–285.

Grabherr MG, et al. 2011. Full-length transcriptome assembly from RNA-Seq data without a reference genome. Nat Biotechnol. 29:644–652.

Gysi DM, et al. 2020. Whole transcriptomic network analysis using Co-expression Differential Network Analysis (CoDiNA). PLoS One. 15:e0240523.

Gysi DM, Voigt A, Fragoso T de M, Almaas E, Nowick K. 2018. wTO: an R package for computing weighted topological overlap and a consensus network with integrated visualization tool. BMC Bioinformatics 19:392.

Huang X, Madan A. 1999. CAP3: a DNA sequence assembly program. Genome Res. 9:868.

Hutchins JRA, et al. 2010. Systematic analysis of human protein complexes identifies chromosome segregation proteins. Science 328:593–599.

Johnson NA, Lachance J. 2012. The genetics of sex chromosomes: evolution and implications for hybrid incompatibility. Ann N Y Acad Sci. 1256:E1–E22.

Katoh K, Misawa K, Kuma K, Miyata T. 2002. MAFFT: a novel method for rapid multiple sequence alignment based on fast Fourier transform. Nucleic Acids Res. 30:3059–3066.

Khaitovich P, et al. 2005. Parallel patterns of evolution in the genomes and transcriptomes of humans and chimpanzees. Science 309:1850–1854.

Kolora SRR, et al. 2018. Divergent evolution in the genomes of closely-related lacertids, *Lacerta viridis* and *L. bilineata* and implications for speciation. GigaScience 8:1–15. doi: 10.1093/gigascience/giy160.

Langfelder P, Horvath S. 2012. Fast R functions for robust correlations and hierarchical clustering. J Stat Softw. 46:i11.

Lechner M, et al. 2011. Proteinortho: detection of (Co-)orthologs in large-scale analysis. BMC Bioinformatics 12:124.

Li H. 2013. Aligning sequence reads, clone sequences and assembly contigs with BWA-MEM. arXiv:1303.3997 [q-bio]. http://arxiv.org/abs/1303.3997 (Accessed July 24, 2019).

Li H, et al. 2009. The Sequence Alignment/Map format and SAMtools. Bioinformatics 25:2078.

Liao Y, Smyth GK, Shi W. 2014. featureCounts: an efficient general purpose program for assigning sequence reads to genomic features. Bioinformatics 30:923–930.

Liu Y, Schröder J, Schmidt B. 2013. Musket: a multistage k-mer spectrum-based error corrector for Illumina sequence data. Bioinformatics 29(3):308–315.

Love MI, Huber W, Anders S. 2014. Moderated estimation of fold change and dispersion for RNA-seq data with DESeq2. Genome Biol. 15:550.

Mack KL, Phifer-Rixey M, Harr B, Nachman MW. 2019. Gene expression networks across multiple tissues are associated with rates of molecular evolution in wild house mice. Genes 10(3):225.

Magoc T, Salzberg SL. 2011. FLASH: fast length adjustment of short reads to improve genome assemblies. Bioinformatics 27(21):2957–2963.

Martin M. 2011. Cutadapt removes adapter sequences from high-throughput sequencing reads. EMBnet J. 17(1):10–12.

Marzahn E, et al. 2016. Phylogeography of the *Lacerta viridis* complex: mitochondrial and nuclear markers provide taxonomic insights. J Zool Syst Evol Res. 54(2):85–105.

Masly JP, Presgraves DC. 2007. High-resolution genome-wide dissection of the two rules of speciation in *Drosophila*. PLoS Biol. 5:e243.

McKenna A, et al. 2010. The genome analysis toolkit: a mapreduce framework for analyzing next-generation DNA sequencing data. Genome Res. 20:1297–1303.

Meyer M, Kircher M. 2010. Illumina sequencing library preparation for highly multiplexed target capture and sequencing. Cold Spring Harb Protoc. 2010:pdb.prot5448.

Mi H, et al. 2010. PANTHER version 7: improved phylogenetic trees, orthologs and collaboration with the Gene Ontology Consortium. Nucleic Acids Res. 38:D204–D210.

Minh BQ, et al. 2020. IQ-TREE 2: new models and efficient methods for phylogenetic inference in the genomic era. Mol Biol Evol. 37(5):1530–1534.

Molnár O, Bajer K, Szövényi G, Török J, Herczeg G. 2016. Space use strategies and nuptial color in European green lizards. herp. 72(1):40–46.

Nowick K, Carneiro M, Faria R. 2013. A prominent role of *KRAB-ZNF* transcription factors in mammalian speciation? Trends Genet. 29:130–139.

Patterson N, et al. 2012. Ancient admixture in human history. Genetics 192:1065–1093.

Pfirrmann T, et al.. 2015. Molecular mechanism of CHRDL1-mediated X-linked megalocornea in humans and in Xenopus model. Hum Mol Genet. 24(11):3119–3132. 10.1093/hmg/ddv063 25712132

Ranwez V, Douzery EJP, Cambon C, Chantret N, Delsuc F. 2018. MACSE v2: toolkit for the alignment of coding sequences accounting for frameshifts and stop codons. Mol Biol Evol. 35:2582–2584.

Rykena S. 1991. Kreuzungsexperimente zur Prüfung der Artgrenzen im Genus Lacerta sensu stricto. Mitt Mus Natkd Berl Zool Reihe. 67(1):55–68.

Sagonas K, et al.. 2014. Molecular systematics and historical biogeography of the green lizards (Lacerta) in Greece: insights from mitochondrial and nuclear DNA. Mol Phylogenet Evol. 76:144–154.

Schilthuizen M, Giesbers MCWG, Beukeboom LW. 2011. Haldane's rule in the 21st century. Heredity. 107:95–102.

Shi C-M, Yang Z. 2018. Coalescent-based analyses of genomic sequence data provide a robust resolution of phylogenetic relationships among major groups of gibbons. Mol Biol Evol. 35:159–179.

Smadja CM, Butlin RK. 2011. A framework for comparing processes of speciation in the presence of gene flow. Mol Ecol. 20:5123–5140.

Storey JD, Bass AJ, Dabney A, Robinson D. 2019. qvalue: Q-value estimation for false discovery rate control. http://github.com/jdstorey/qvalue. Accessed August 14, 2019.

Sudmant PH, Alexis MS, Burge CB. 2015. Meta-analysis of RNA-seq expression data across species, tissues and studies. Genome Biol. 16:287.

Tollis M, et al. 2018. Comparative genomics reveals accelerated evolution in conserved pathways during the diversification of anole lizards. Genome Biol Evol. 10:489–506.

Uebbing S, et al. 2016. Divergence in gene expression within and between two closely related flycatcher species. Mol Ecol. 25(9):2015–2028.

Voolstra C, Tautz D, Farbrother P, Eichinger L, Harr B. 2007. Contrasting evolution of expression differences in the testis between species and subspecies of the house mouse. Genome Res. 17:42–49.

Wang D, Zhang Y, Zhang Z, Zhu J, Yu J. 2010. KaKs_Calculator 2.0: a toolkit incorporating gamma-series methods and sliding window strategies. Genomics Proteomics Bioinformatics. 8:77–80.

Wang Z-Y, et al. 2020. Transcriptome and translatome co-evolution in mammals. Nature. 588:642–647.

Wilson Sayres MA. 2018. Genetic diversity on the sex chromosomes. Genome Biol Evol. 10:1064–1078.

Wu TD, Reeder J, Lawrence M, Becker G, Brauer MJ. 2016. GMAP and GSNAP for genomic sequence alignment: enhancements to speed, accuracy, and functionality. In: Mathé E, Davis S, editors. Statistical genomics: methods and protocols. Methods in molecular biology. New York (NY): Springer. p. 283–334. doi:10.1007/978-1-4939-3578-9_15.

Yoder AD, et al. 2016. Geogenetic patterns in mouse lemurs (genus Microcebus) reveal the ghosts of Madagascar's forests past. PNAS. 113:8049–8056.

Zhao L, Wit J, Svetec N, Begun DJ. 2015. Parallel gene expression differences between low and high latitude populations of *Drosophila melanogaster* and *D. simulans*. PLOS Genet. 11:e1005184.

**Associate editor:** Jay Storz